

Fragmentation functions and parton distribution functions for the pion with the nonlocal interactions

Seung-il Nam^{1,*} and Chung-Wen Kao^{2,†}

¹*School of Physics, Korea Institute for Advanced Study (KIAS), Seoul 130-722, Korea*

²*Department of Physics, Chung-Yuan Christian University (CYCU), Chung-Li 32023, Taiwan*

(Dated: May 16, 2022)

We study the unpolarized fragmentation functions and parton distribution functions of the pion employing the nonlocal chiral quark model. This model manifests the nonlocal interactions between the quarks and pseudoscalar mesons in the light-cone coordinate. It turns out that the nonlocal interactions generate substantial changes in comparison to typical models with only local couplings. We also perform the high Q^2 -evolution for our results calculated at a relatively low renormalization scale $Q^2 \approx 0.36 \text{ GeV}^2$, in order to compare them with the experimental data. Our results after evolution are in qualitatively good agreement with those data.

PACS numbers: 12.38.Lg, 13.87.Fh, 12.39.Fe, 14.40.-n, 11.10.Hi.

Keywords: Unpolarized fragmentation and quark distribution functions, pseudoscalar meson, nonlocal chiral-quark model, DGLAP evolution.

I. INTRODUCTION

To apply perturbative Quantum Chromodynamics (QCD) to hadronic physics, one needs the QCD factorization theorem to guarantee the cross section to be the convolution of the two parts: the process-dependent perturbative QCD (pQCD) calculable short-distance parton cross section, and the universal long-distance functions which can be extracted from experiments. Since the strong interaction in long-distance is essentially nonperturbative, those long-distance functions are incalculable by pQCD.

To date, there has been increasing interest in those long-distance functions such as the fragmentation functions and parton distribution functions. The fragmentation function characterizes the probability for a hadron fragmented from a quark with the momentum fraction z . It plays a crucial role in analyzing the semi-inclusive processes in the electron-positron scattering, deep-inelastic proton-proton scattering, and so on [1–4]. The parton distribution function provides information for the distribution of the momentum fraction x carried by a parton inside a hadron. It is necessary ingredient in studying hard scattering processes such as the deep-inelastic electron-proton scattering. It is worth mentioning that a parton distribution function can be extracted from the corresponding fragmentation function via the Drell-Levi-Yan (DLY) relation due to the analytical continuation [5].

Because of these salient physical meanings implied in those functions, they have been intensively studied [6–23]. These functions have been extracted from the available empirical data by global analyses or from the parametrizations which satisfy certain constraints [6–10]. Theoretically many investigations on the fragmentation functions have carried out. For example, a rigorous QCD proof has done for the momentum sum rules of the fragmentation functions [14]. The Dyson-Schwinger method was applied to compute the valance-quark distribution function, resulting in relatively good agreement with the available experimental data for the pion and kaon [18]. Monte-Carlo simulations with supersymmetric (SUSY) QCD were carried out to obtain the fragmentation function up to a very high \sqrt{s} [19]. The authors of Refs. [20–23] have also made use of the instanton-motivated approaches to compute the quark distribution function as well.

Among those approaches, we are in particular interested in the ones based on the chiral dynamics. Because the strong interaction in long-distance is dominated by the chiral physics, therefore the nonperturbative objects such as fragmentation functions should be also subjected to the chiral physics. Along this line, the fragmentation functions were first studied by Georgi-Manohar model in [11] and later by chiral-quark-meson coupling models in the pseudoscalar (PS) and pseudovector (PV) schemes [12, 13]. Their results indicate considerable differences between two schemes. In Refs. [15–17], the authors studied the fragmentation functions for various hadrons in terms of the Nambu-Jona-Lasinio (NJL) model. In their works, hadron jets and resonances were taken into account additionally

*E-mail: sinam@kias.re.kr

†E-mail: cwkao@cycu.edu.tw

such that the momentum sum rule is satisfied. The hadron-jet contributions turned out to be essential to reproduce the various fragmentation functions for the small z region.

In the present work, we concentrate on the fragmentation functions and quark distribution functions for the SU(2) light flavor for the positively charged pion, i.e. $\pi^+ \equiv u\bar{d}$. We only evaluate the π^+ case because the other isospin channels can be easily obtain by multiplying the corresponding isospin factors [17]. For this purpose, we employ the nonlocal chiral quark model (NLChQM). This model is based on the dilute instanton-liquid model (LIM) [24–28]. It is worth mentioning that, NLChQM have successfully produced results for various physical quantities which are in agreement with experiments as well as lattice QCD (LQCD) simulations. [29–34].

Our calculations are performed in the light-cone coordinate at a relatively low renormalization scale $\mu \approx 0.6$ GeV, corresponding to the average size of the (anti)instanton $\bar{\rho} \approx 1/3$ fm and average inter-instanton distance $\bar{R} \approx 1$ fm for the dilute (anti)instanton ensemble. These instanton parameters have been determined phenomenologically [24] or generated by LQCD simulations [35]. Although the fragmentation and the parton distribution functions are defined properly only in Minkowski space and there has been no rigor proof, we still assume that there is an appropriate analytic continuation between the instanton physics and the NLChQM defined in the light-cone coordinate. We notice that there have been successful applications based on this assumption to various physical quantities [20–23].

Distinctive features of the present approach, in comparison to other *local* effective chiral models such as the conventional NJL model and usual quark-meson coupling models, are as follows: 1) The couplings between quarks and pseudoscalar (PS) mesons are nonlocal. Those nonlocal interactions are led by the intricate quark-(anti)instanton interactions inside the instanton ensemble, flipping quark helicities [24–28]. 2) As a result, the quark-PS meson coupling, which is represented by the momentum-dependent constituent-quark mass, plays the role of the natural UV regulator. Hence, one does not need any artificial regulators. Interestingly enough, the computed momentum-dependence of the mass turns out to be very comparable with the LQCD simulations [28, 36]. 3) Moreover, all the relevant physical quantities such as the low-energy constants (LECs) are determined self-consistently with only two phenomenological parameters, i.e. average (anti)instanton size ($\bar{\rho}$) and inter-(anti)instanton distance (\bar{R}). There is no more free adjustable free parameters within the framework as long as we are involved in the light-flavor SU(2) sector. We emphasize that, among the above features, the nonlocality of the interaction is the most important ingredient which has never appeared in other chiral models.

As for the numerical calculations, we compute the *elementary* fragmentation function $zd_u^\pi(z)$, standing for the fragmentation process $u \rightarrow \pi q'$, where π is assigned for π^+ throughout this work, i.e. the quark u quark is fragmented into the pion and an energetic quark q' . Since an energetic quark will be fragmented into other hadrons until it possesses insufficient energy to be fragmented into hadrons, this elementary fragmentation function does not satisfy the momentum sum rule [16, 17]. It is likely that if the hadron jets and resonance contributions are taken into account, the sum rule will be satisfied [16, 17]. However we will not consider those effects for brevity in the present work. Our results of the fragmentation functions turn out to be substantial larger in comparison to other models and more symmetric over the momentum fraction z . This observation can be understood by the nonlocal quark-PS meson coupling structure discussed in detail in Section III.

The elementary fragmentation function is modified into the *renormalized* one, i.e. $zd_u^\pi(z) \rightarrow zD_u^\pi(z)$. This is due to the fact that the meson-cloud effects enhance the elementary fragmentation functions [15, 16]. We find that such enhancements are relatively small in the present model: If we compare the effects with those from other models, they show about 80 ~ 90% of the renormalized fragmentation function comes from the meson-cloud effects. On the other hand, only about 60% in the present model. In other words, the nonlocal couplings between quarks and PS mesons in our model somehow mimic part of the meson-cloud effects. Therefore our "elementary" fragmentation functions have already contained more pion-cloud contribution than other models.

The calculated fragmentation functions are evolved to high Q^2 by the DGLAP evolution using the parton-cascade code *QCDNUM* [37, 38] to compare with the empirical data. By doing so, we see qualitative agreement between our result and the empirical data, although some underestimates are shown in the small- z region. This defect is expected to be improved by the inclusion of the hadron-jet contributions [16, 17].

The parton distribution function $xf_u^\pi(x)$ is extracting from the fragmentation function by the DLY relation. Similarly we obtain a more symmetric curve of the parton distribution function in comparison to the NJL model [16, 17]. As done in Refs. [16, 17], we provide the numerical results for the minus-type and plus-type quark distribution functions, i.e. $x(f_u^\pi - f_{\bar{u}}^\pi)$ and $x(f_u^\pi + f_{\bar{u}}^\pi)$, respectively. Note that the minus-type one is nothing but the valance quark-distribution function. Again, we perform the high Q^2 evolution in order to compare our results with the empirical ones, resulting in qualitative agreement except the sizable underestimate observed again in the small- x region after the evolution up to $Q^2 = 4 \text{ GeV}^2$ for the minus-type one. This discrepancy may ask more realistic treatments beyond the elementary process, such as the hadron-jet contributions as mentioned previously. The high Q^2 evolution up to $Q^2 = 27 \text{ GeV}^2$ reproduces the experimental data qualitatively well.

The present report is structured as follows: In Section II, we briefly introduce the model we use and sketch our computation procedure. In Section III we present our numerical results and related discussions. The final Section is

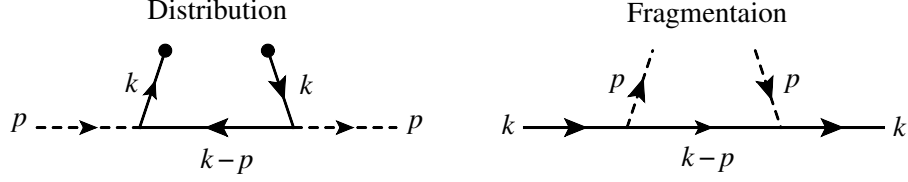


FIG. 1: Schematic figures for the quark-distribution (left) and fragmentation (right) functions, in which the solid and dash lines denote the quark and pseudoscalar meson, respectively.

devoted for the summary, conclusion, and future perspectives.

II. NONLOCAL PION-QUARK COUPLING

The unpolarized fragmentation function D_q^h indicates the process that an off-shell quark (q) is fragmented into an unobserved particle (X) and on-shell hadron (h), i.e. $q \rightarrow hX$. A schematic figure for this function is given in the right of Figure 1. Here, the fragmentation function is defined in the light-cone coordinate, assuming the light-cone gauge, as follows [12, 13]:

$$D_q^h(z, k_T^2, \mu) = \frac{1}{4z} \int dk^+ \text{Tr} [\Delta(k, p, \mu) \gamma^-] |_{zk^- = p^-}, \quad (1)$$

where k , p and z stands for the four momenta of the initial quark and fragmented hadron, and the longitudinal momentum fraction possessed by the hadron, respectively. k_\pm denotes $(k_0 \pm k_3)/\sqrt{2}$ in the light-cone coordinate. k_T and μ denotes the transverse momentum of the quark and the renormalization scale at which the fragmentation process computed. Note that we consider this renormalization scale is almost the same with the momentum-transfer scale, i.e. $\mu^2 \approx Q^2$, unless otherwise stated. The correlation $\Delta(k, p, \mu)$ reads generically:

$$\Delta(k, p, \mu) = \sum_X \int \frac{d^4\xi}{(2\pi)^4} e^{+ik \cdot \xi} \langle 0 | \psi(\xi) | h, X \rangle \langle h, X | \psi(0) | 0 \rangle. \quad (2)$$

Here ψ represents the quark field, whereas ξ the spatial interval on the light cone. Furthermore one can integrate over k_\perp ,

$$D_q^h(z, \mu) = \pi \int_0^{K_{\max}^2} dk_T^2 D_q^h(z, k_T, \mu). \quad (3)$$

Here K_{\max}^2 stands for the cutoff mass of the transverse momentum. The integrated fragmentation function satisfies the momentum sum rule:

$$\int_0^1 \sum_h D_q^h(z, \mu) dz = 1, \quad (4)$$

where h indicates for all the possible hadrons fragmented. Eq. (4) means that all of the momentum of the initial quark q is transferred into the momenta of the fragmented hadrons. From the Drell-Levi-Yan (DLY) relation [5, 13, 15–17], D_q^h can be related to the parton distribution function f_q^h , provided that there is a proper analytic continuation. The relation is as follows,

$$D_q^h(z) = \frac{z}{6} f_q^h(x), \quad \text{where } x = \frac{1}{z}, \quad (5)$$

where x denotes the momentum fraction possessed by a parton inside the hadron. A schematic figure for the quark-distribution function is depicted in the left of Figure 1.

In this article, we use NLChQM to investigate these nonperturbative objects, i.e. fragmentation and parton distribution functions. This model is motivated from the dilute instanton liquid model [24–28]. We note that, to date, various nonperturbative QCD properties have been well studied in terms of the instanton vacuum configuration and the results are comparable with experiments and LQCD simulations [29–32]. In that model, nonperturbative

QCD effects are deciphered by the nontrivial quark-instanton interactions in the dilute instanton ensemble. However this model by nature is defined in Euclidean space because the (anti)instantons are well defined there by signaling the tunneling between the infinitely degenerate QCD vacua. Although there have been no rigor derivation on the analytic continuation from the instanton physics to those in Minkowski one, there are still several challenging studies which try to apply the idea of the instanton physics to the physical quantities defined properly only in Minkowski space, such as the light-cone wave function [20–23]. Following those studies we adopt the effective chiral action (EChA) from NLChQM in Minkowski space as follows:

$$\mathcal{S}_{\text{eff}}[m_f, \phi] = -\text{Sp} \ln \left[i\rlap{\not{\partial}} - \hat{m}_f - \sqrt{M(\overleftarrow{\partial}^2)} U^{\gamma_5} \sqrt{M(\overrightarrow{\partial}^2)} \right], \quad (6)$$

where Sp and \hat{m}_f denote the functional trace $\text{Tr} \int d^4x \langle x | \cdots | x \rangle$ over all the relevant spin spaces and $\text{SU}(2)$ current-quark mass matrix $\text{diag}(m_u, m_d)$, respectively. Throughout the present work, we will take $m_u = m_d = 5$ MeV. Note that, in deriving EChA in Eq. (6), we simply replace the Euclidean metric for the (anti)instanton effective chiral action into that for Minkowski space. The momentum-dependent effective quark mass generated from the interactions between the quarks and nonperturbative QCD vacuum, can be written in a simple n -pole type form factor as follows [20–23]:

$$M(\partial^2) = M_0 \left[\frac{n\Lambda^2}{n\Lambda^2 - \partial^2 + i\epsilon} \right]^n, \quad (7)$$

where n indicates a positive integer number. We will take $n = 2$ as in the instanton model [22, 23]. Λ stands for the model renormalization scale. It is related to the average (anti)instanton size $\bar{\rho}$. We will discuss this scale issue more in Section III. The nonlinear PS-meson field, i.e. U^{γ_5} takes a simple form [28] with the normalization following Ref. [12] to be consistent with the definition of the fragmentation function in Eq. (1):

$$U^{\gamma_5}(\phi) = \exp \left[\frac{i\gamma_5(\boldsymbol{\tau} \cdot \boldsymbol{\phi})}{2F_\phi} \right] = 1 + \frac{i\gamma_5(\boldsymbol{\tau} \cdot \boldsymbol{\phi})}{2F_\phi} - \frac{(\boldsymbol{\tau} \cdot \boldsymbol{\phi})^2}{8F_\phi^2} + \cdots, \quad (8)$$

where F_ϕ stands for the weak-decay constant for the PS meson ϕ . For instance, F_π is chosen to be about 93 MeV in this normalization. We also write explicitly

$$\boldsymbol{\tau} \cdot \boldsymbol{\phi} = \begin{pmatrix} \pi^0 & \sqrt{2}\pi^+ \\ \sqrt{2}\pi^- & -\pi^0 \end{pmatrix}. \quad (9)$$

By expanding the nonlinear PS-meson field up to $\mathcal{O}(\phi^1)$ from EChA in Eq. (6), one can derive the following effective interaction Lagrangian density for the nonlocal quark-quark-PS meson vertex:

$$\mathcal{L}_{\phi qq} = \frac{i}{2F_\phi} \bar{q} \sqrt{M(\overleftarrow{\partial}^2)} \gamma_5 (\boldsymbol{\tau} \cdot \boldsymbol{\phi}) \sqrt{M(\overrightarrow{\partial}^2)} q. \quad (10)$$

Then, the correlation in Eq. (2) can be evaluated using this effective Lagrangian for the *elementary* fragmentation function $q(k) \rightarrow \phi(p) + q'(r)$:

$$\begin{aligned} \Delta(k, p, \mu) &= -\frac{1}{(2\pi)^4} \frac{M_k M_r}{2F_\phi^2} \left(\frac{\not{k} + \bar{M}_k}{k^2 - \bar{M}_k^2} \right) \gamma_5 (\not{k} - \not{p} + \bar{M}_r) \gamma_5 \left(\frac{\not{k} + \bar{M}_k}{k^2 - \bar{M}_k^2} \right) [2\pi\delta(r^2 - \bar{M}_r^2)], \\ &\approx -\frac{1}{(2\pi)^4} \frac{M_k M_r}{2F_\phi^2} \left(\frac{\not{k} + \bar{M}_f}{k^2 - \bar{M}_f^2} \right) \gamma_5 (\not{k} - \not{p} + \bar{M}_{f'}) \gamma_5 \left(\frac{\not{k} + \bar{M}_f}{k^2 - \bar{M}_f^2} \right) [2\pi\delta(r^2 - \bar{M}_{f'}^2)], \end{aligned} \quad (11)$$

where the momentum-dependent effective quark mass is written via Eq. (7):

$$M_\ell = M_0 \left[\frac{2\Lambda^2}{2\Lambda^2 - \ell^2 + i\epsilon} \right]^2. \quad (12)$$

In Eq. (11) we adopt the following notations: $\bar{M}_\ell \equiv m_f + M_\ell$ and $\bar{M}_{f'} \equiv m_f + M_0$. Note that f and f' indicate the flavors for the initial (q) and final (q') quarks, respectively. Eq. (11) stands for the π^+ elementary fragmentation, i.e. $u \rightarrow \pi^+ d$. As for the fragmentation of a neutral pion, one needs multiply a factor 1/2 to Eq. (11). From the first line to the second line in Eq. (11), we approximate the momentum-dependent effective quark mass into a constant constituent-quark mass in the denominator $M_\ell \rightarrow M_0$, since the momentum dependencies from those mass terms in

the denominator play only minor roles numerically. Moreover, this approximation simplifies the numerical calculations to a great extent. Performing the trace over the Lorentz indices for the fragmentation function in Eq. (1):

$$\text{Tr}[(\not{k} + \bar{M}_f) \gamma_5 (\not{k} - \not{p} + \bar{M}_{f'}) \gamma_5 (\not{k} + \bar{M}_f) \gamma_\mu] = -4 [p_\mu(k^2 - \bar{M}_f^2) + k_\mu(\bar{M}_f^2 - 2\bar{M}_f\bar{M}_{f'} + k^2 - 2k \cdot p)], \quad (13)$$

we reach a concise expression for the elementary fragmentation function $u \rightarrow \pi^+ d$ from NLChQM:

$$d_u^{\pi^+}(z, k_T^2, \mu) = \frac{1}{8\pi^3 z(1-z)} \frac{M_k M_r}{2F_\phi^2} \left[\frac{z(k^2 - \bar{M}_f^2) + (k^2 + \bar{M}_f^2 - 2\bar{M}_f\bar{M}_{f'} - 2k \cdot p)}{(k^2 - \bar{M}_f^2)^2} \right], \quad (14)$$

where the relevant four momenta squared in the present theoretical calculations are defined in the light-cone coordinate as follows:

$$k^2 = k_+ k_- - k_T^2, \quad r^2 = (k - p)^2 \approx k_+ k_- - k_T^2 + m_\phi^2 - (k_+ p_- + k_- p_+),$$

where we have ignored the transverse PS-meson momentum on the light cone, i.e. $p_T \approx 0$.

Since we are interested in the pion case in the present work, the value of M_0 is determined to reproduce the appropriate value for the pion weak-decay constant $F_\pi \approx 93$ MeV through the light-cone wave function calculations [20–23], resulting in $M_0 \approx 350$ MeV with $\Lambda = 1/\bar{\rho} \approx 600$ MeV. Note that this value of M_0 also can be determined self-consistently within the instanton model [24–32] with the phenomenological (anti)instanton parameters $\bar{\rho} \approx 1/3$ fm and $\bar{R} \approx 1$ fm, which is the average inter-instanton distance. Note that this quantity is a function of (z, m_π^2, k_T^2) in general. Note that the pion mass is chosen to be $m_\pi = 140$ MeV. Collecting all the ingredients above, one is led to a final expression for the elementary fragmentation function:

$$d_u^{\pi^+}(z, k_T^2, \mu) = \frac{1}{8\pi^3} \frac{M_k M_r}{2F_\phi^2} \frac{z [z^2 k_T^2 + [(z-1)\bar{M}_f + \bar{M}_{f'}]^2]}{[z^2 k_T^2 + z(z-1)\bar{M}_f^2 + z\bar{M}_{f'}^2 + (1-z)m_\pi^2]^2}, \quad (15)$$

where M_k and M_r are the momentum-dependent quark mass manifesting the nonlocal quark-PS meson interactions, read:

$$M_k = \frac{M_0 [2\Lambda^2 z(1-z)]^2}{[z^2 k_T^2 + z(z-1)(2\Lambda^2 - \delta^2) + z\bar{M}_f^2 + (1-z)m_\pi^2]^2}, \quad M_r = \frac{M_0 (2\Lambda^2)^2}{(2\Lambda^2 - \bar{M}_{f'}^2)^2}. \quad (16)$$

As for M_k in Eq. (16), we have introduced a free and finite-valued parameter δ in the denominator to avoid the unphysical singularities, which appear in the vicinity of $(z, k_T) = 0$, due the present parameterization of the effective quark mass as in Eq. (7). We determine δ to satisfy a natural conditions for all the possible values of (z, k_T) :

$$|z^2 k_T^2 + z(z-1)(n\Lambda^2 - \delta^2) + z\bar{M}_f^2 + (1-z)m_\pi^2| > 0. \quad (17)$$

It is easy to see that one of the trivial solutions for Eq. (17) can be $\delta^2 = n\Lambda^2 - \bar{M}_f^2$, considering the quark propagator in Eq. (15). Although there can be other solutions, we will use this value for δ for the fragmentation function as a trial hereafter. Physically, those unphysical singularities can be understood as that a hypothetic particle, whose mass corresponds to $\sqrt{2}\Lambda$, becomes its on-mass shell for a certain combination of (z, k_T) . Thus, we employed δ to exclude that unphysical situation. We also verified that the change of δ does not make considerable effects on the numerical results, as far as Eq. (17) is fulfilled.

If we replace all the momentum-dependent masses into a constant one M in Eqs. (15) and (16) in the chiral limit, and change the quark-PS meson coupling into a constant one appropriately in Eq. (15), we obtain the expression for the elementary fragmentation function from the quark-meson coupling model [13] :

$$d_u^{\pi^+}(z, k_T^2, \mu) = \frac{1}{8\pi^3} g_{\phi qq}^2 \frac{z(z^2 k_T^2 + z^2 M^2)}{[z^2 k_T^2 + z^2 M^2 + (1-z)m_\pi^2]^2}. \quad (18)$$

The above equation is also equivalent with that from the NJL model calculations in principle [15–17]. Note that the on-shell value of $M_0^2/(2F_\pi^2)$ becomes about 7, which is quite similar to $g_{qq\pi}^2 \approx 9$, used in Refs. [13, 15–17]. The elementary fragmentation function can be evaluated further by integrating Eq. (15) over k_T as:

$$d_u^{\pi^+}(z, \mu) = 2\pi z^2 \int_0^\infty d_{q,\bar{q}}^\phi(z, k_T^2, \mu) k_T dk_T, \quad (19)$$

where the renormalization scale is set to be $\mu \approx \Lambda = 600$ MeV for the numerical calculations. We will present the numerical results for Eq. (19) in the next Section.

Using the DLY relation in Eq. (5), one can derive the quark-distribution function for π^+ , i.e. $f_u^{\pi^+}$ as follows:

$$f_u^{\pi^+}(x, k_T^2, \mu) = \frac{3}{4\pi^3} \frac{\mathcal{M}_k \mathcal{M}_r}{2F_\phi^2} \frac{k_T^2 + [(x-1)\bar{M}_f - x\bar{M}_{f'}]^2}{[k_T^2 + (1-x)\bar{M}_f^2 + x\bar{M}_{f'}^2 + x(x-1)m_\pi^2]^2}, \quad (20)$$

where we have defined the effective quark masses for the quark distribution function by

$$\mathcal{M}_k = \frac{4M_0\Lambda^4(1-x)^2}{[k_T^2 + (1-x)(2\Lambda^2) + x\bar{M}_{f'}^2 + x(x-1)m_\pi^2]^2}, \quad \mathcal{M}_r = \frac{4M_0\Lambda^4}{(2\Lambda^2 - \bar{M}_{f'}^2)^2}. \quad (21)$$

Note that \mathcal{M}_k in Eq. (21) does not suffer from the unphysical singularities unlike that in Eq. (16), according to the different kinematic situations between those functions. Again, if we take the replacements as $\bar{M}_{f,f'} \rightarrow M$ and $\mathcal{M}_k \mathcal{M}_r / (2F_\pi^2) \rightarrow g_{\phi qq}^2$ as done for the fragmentation function, one is led to

$$f_u^{\pi^+}(x, k_T^2, \mu) = \frac{3}{4\pi^3} g_{\phi qq}^2 \frac{k_T^2 + M^2}{[k_T^2 + M^2 + x(x-1)m_\pi^2]^2}, \quad (22)$$

which is equivalent to Eq. (14) in Ref. [16] in the chiral limit. Similarly, the integration over k_T can be performed as follows, resulting in a function of x at a certain renormalization scale $\mu \approx \Lambda$:

$$f_u^{\pi^+}(x, \mu) = 2\pi \int_0^\infty f_{q,\bar{q}}^\phi(z, k_T^2, \mu) k_T dk_T. \quad (23)$$

We will use the notation π instead of π^+ from now on for convenience.

III. NUMERICAL RESULTS

Here we present our numerical results for the fragmentation functions and parton distribution functions of π with relevant discussions. We will consider only the favored fragmentation process $u\pi \rightarrow d$. As in the instanton model the value of Λ is proportional to $1/\bar{\rho}$ giving the renormalization scale $\Lambda \approx 600$ MeV as mentioned in the previous Section. However, the cutoff mass for k_T is usually determined by the Lepage-Brodsky (LB) regularization scheme [39] for the fragmentation function in many local models [13, 15–17]. Hence, even this UV divergence can be tamed by the momentum-dependent effective quark mass in Eq. (12) in our work, we take into account two different models depending on how to treat the value of Λ :

- Model I: The value of Λ is determined by the phenomenological instanton parameter, i.e. $\Lambda \approx 600$ MeV, and the integration over k_T in Eq. (18) is performed for $0 \leq k_T \leq \infty$.
- Model II: The cutoff mass for k_T is determined by the LB scheme, while Λ is the same with that of Model I, and the integration over k_T in Eq. (18) is performed for $0 \leq k_T \leq \Lambda_{\text{LB}}$.

The value of Λ_{LB} is computed by [17]:

$$\Lambda_{\text{LB}}^2 = z(1-z) \left(\sqrt{\Lambda^2 + m_\pi^2} + \sqrt{\Lambda^2 + M_0^2} \right)^2 - (1-z)m_\pi^2 - zM_0^2. \quad (24)$$

First, we present the numerical results for the elementary fragmentation functions zd_u^π as functions of z in the left panel of Figure 2 for Model I (solid), II (dotted), NJL (dashed), PS (long-dashed), and PV (dotted-dashed) results. As for the NJL result, the renormalization scale is chosen to be 0.18 GeV^2 as usual [13, 15–17], whereas it becomes 1 GeV^2 for the PS and PV schemes of the quark-meson coupling model [13]. From the left panel of Figure 2, we observe that our curves are in general much larger than other model results. Moreover, while the peaks of the curves locate at $z \sim 0.5$ for the present theoretical framework, the maximum values of NJL and PS scheme are around $z \sim 0.7$. On the other hand, the maximum value occurs in PV scheme at the location where is close to ours. The behaviors of the NJL and PS-scheme curves are similar (equivalent) to each other is because they are both local models without derivatives.

Note that these elementary fragmentation functions computed here do not satisfy the momentum sum rule, which is defined in Eq. (4). Since we have considered the elementary process $q \rightarrow \pi q'$, however, as discussed in Refs. [16, 17], the pion-cloud effects can enhance the elementary fragmentation function, and those fragmentation functions with the

pion-cloud effects were identified as the *renormalized* fragmentation function. The pion-cloud effects can be estimated by the renormalization factor, defined by

$$\mathcal{N}_{\pi/u} \equiv \sum_{\pi} \int_0^1 dz d_u^{\pi}(z) \ll 1. \quad (25)$$

where the summation runs over the all isospin states of the PS meson. It is worth mentioning that $\mathcal{N}_{\phi/q}$ is the same quantity with $(1 - Z_Q)$ in Ref. [16]. For instance, in Refs. [16, 17], the value of $\mathcal{N}_{\pi/q}$ was estimated to be $(0.1 \sim 0.2)$. As understood, this smallness of $\mathcal{N}_{\pi/q}$ results in the breakdown of the momentum sum rule. The renormalized fragmentation function then can be defined as [16]:

$$D_u^{\pi}(z) \approx \frac{d_u^{\pi}(z)}{\sum \mathcal{N}_{\pi/u}}. \quad (26)$$

Here, we note that the summation runs over all the possible fragmented hadron states from the u quark in principle. However, since we are interested only in the pion case, we restrict ourselves to the SU(2) light-flavor mesons, i.e. no kaons. From the numerical computations, we obtain

$$\mathcal{N}_{\pi/u}^{\text{Model I}} = 0.3685, \quad \mathcal{N}_{\pi/u}^{\text{Model II}} = 0.4120, \quad \mathcal{N}_{\pi/u}^{\text{NJL}} = 0.0257, \quad \mathcal{N}_{\pi/u}^{\text{PS}} = 0.0843, \quad \mathcal{N}_{\pi/u}^{\text{PV}} = 0.1684. \quad (27)$$

From the values in Eq. (27), we find that Model I and II give much larger results compared with those in the models with local interactions. This observation tells us that the probability for the initial quark to be fragmented into the hadrons, especially pion, turns out to be much higher due to the nonlocal interactions. Physically, this enhancement of $\mathcal{N}_{\pi/q}$ can be understood in the following way: The nonlocal interactions are originally generated from the intricate quark-(anti)instanton interactions in the instanton-vacuum picture [24–28]. This momentum-dependent quark mass can be understood as a dressed-quark mass as in usual Dyson-Schwinger methods [18] where the quarks are dressed by the pion cloud. In this sense, the nonlocal interaction represented by the momentum-dependent effective quark mass practically contains considerable contributions from the pion cloud. It leads to the higher probabilities for the initial quark to be fragmented into the pion, comparing to usual local models with a constant quark mass and coupling. The numerical results for the renormalized fragmentation functions are given in the right panel of Figure 2. Interestingly, the $zD_u^{\pi}(z)$ curves from the present nonlocal model calculations look like an average of the PS- (or NJL) and PV-scheme results. This can be understood qualitatively by expanding the momentum-dependent quark masses of $\sqrt{M_k M_r} \sim M_k$ in Eq. (12):

$$M_k \approx M_0 - M_0 \frac{k^2}{\Lambda^2} + \dots. \quad (28)$$

The first term of Eq. (28) relates to the PS scheme (or NJL) without derivatives, while the second term to the PV one with derivatives, qualitatively. In this way, the present result can be seen as sort of a mixture of the two coupling models. We also find that the curves from Model I and II are very similar to each other.

The numerical results for the parton distribution functions in Eq. (23) are given in Figure 3 for Model I (solid), II (dotted) and NJL (dashed) cases as functions of the momentum fraction x possessed by a quark inside the meson. All the calculations are carried out at the same renormalization scales as for the fragmentation functions. Here is one caveat: In plotting the quark distribution curve for Model II, we used the same Λ_{LB} with that for the fragmentation function for brevity, although the analytic expression for Λ_{LB} in Eq. (24) would be changed by the DLY relation. From Figure 3, obvious similarities are observed between the curves for Model I and II. Both of them are very symmetric and peak at $x \approx 0.5$. The NJL result is tilted to the region near $x = 1$. Thus, we can conclude that the nonlocal interactions between the quark and PS meson effects much on the shape of the quark-distribution-function curves in comparison to those from the local model calculations, as already observed in the fragmentation functions in Figure 2. According to Ref. [10], the quark distribution functions can be parameterized by the following forms:

$$\begin{aligned} x f_u^{\pi}(x) &= x f_d^{\pi}(x) = A_v^{\pi} x^{\alpha_{\pi}} (1-x)^{\beta_{\pi}} : \text{quark contribution,} \\ x f_{\bar{u}}^{\pi}(x) &= x f_{\bar{d}}^{\pi}(x) = \frac{1}{6} A_s^{\pi} (1-x)^{\eta_{\pi}} : \text{antiquark contribution,} \end{aligned} \quad (29)$$

where we have assumed that SU(2) flavor symmetry for the valance and sea quarks, respectively. Using Eq. (29), $x f_u^{\pi}(x)$ in Figure 3 can be parameterized at $Q^2 = 0.36 \text{ GeV}^2$ and the fitted values for A_v^{π} , α_{π} , and β_{π} are listed in Table I. These parameterized distribution functions will be used for the inputs for the high- Q^2 evolution. To compare with the empirical data obtained in Ref. [7], we need execute the high- Q^2 evolution of our calculation results. For this purpose, we will make use of the numerical DGLAP evolution code *QCDNUM17* by Botje [37, 38].

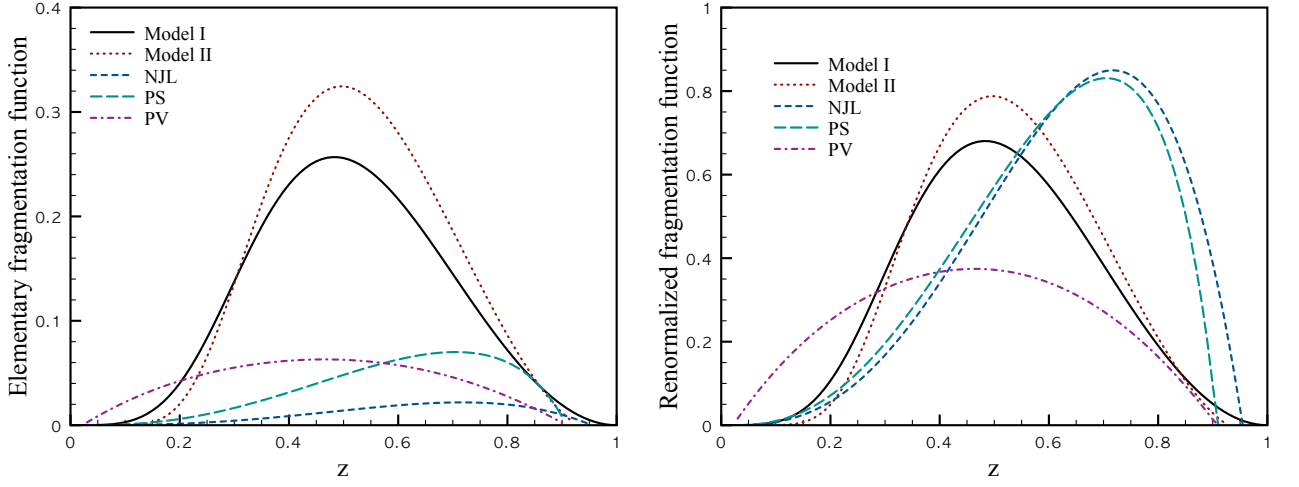


FIG. 2: (Color online) In the left panel, we show elementary fragmentation functions $zd_u^\pi(z)$ at low renormalization scale for model I ($Q^2 = 0.36 \text{ GeV}^2$, solid), model II ($Q^2 = 0.36 \text{ GeV}^2$, dot), NJL [16, 17] ($Q^2 = 0.18 \text{ GeV}^2$, dash), PS scheme [12, 13] ($Q^2 = 1 \text{ GeV}^2$, long-dash), and PV scheme [12, 13] ($Q^2 = 1 \text{ GeV}^2$, dot-dash). Renormalized elementary fragmentation functions $zD_u^\pi(z)$ by Eq. (26) are also shown in the right panel in the same manner with the left panel.

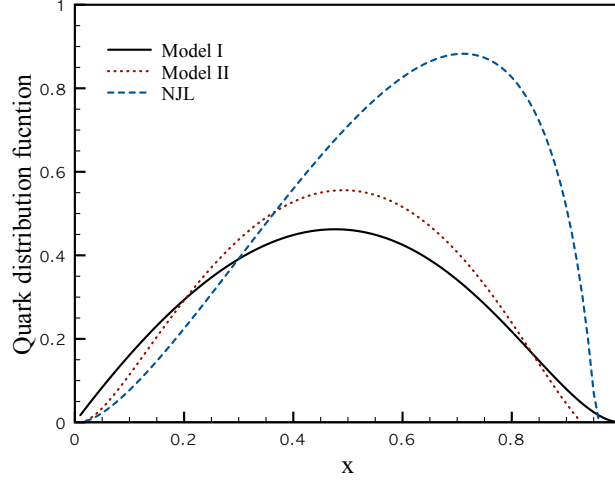


FIG. 3: (Color online) Quark distribution functions $xf_u^\pi(x)$ computed using model I (solid), model II (dot), and NJL [16, 17] (dash) at low Q^2 values: $Q^2 = 0.36 \text{ GeV}^2$ for the present models and $Q^2 = 0.18 \text{ GeV}^2$ for the NJL.

The quark distribution functions computed and parameterized previously becomes the inputs for the evolution. For the QCDNUM evolution, one needs three valance quark $x(q - \bar{q})$ and anti-quark $x\bar{q}$ distributions. First, in Figure 4, we show the numerical results for the renormalized fragmentation functions for Model I (left) and II (right) cases, evolved from $Q^2 = 0.36 \text{ GeV}^2$ (solid) to $Q^2 = 1 \text{ GeV}^2$ at LO (dot) evolution. The empirical fragmentation function is

$Q^2 = 0.36 \text{ GeV}^2$	A_v^π	α_π	β_π
Model I	2.8736	1.2163	1.4280
Model II	6.2030	1.6669	1.7074
NJL	5.2497	1.9131	0.9208

TABLE I: Fitted values for the quark distribution function, A_v^π , α_π , and β_π in Eq. (29) at $Q^2 = 0.36 \text{ GeV}^2$.

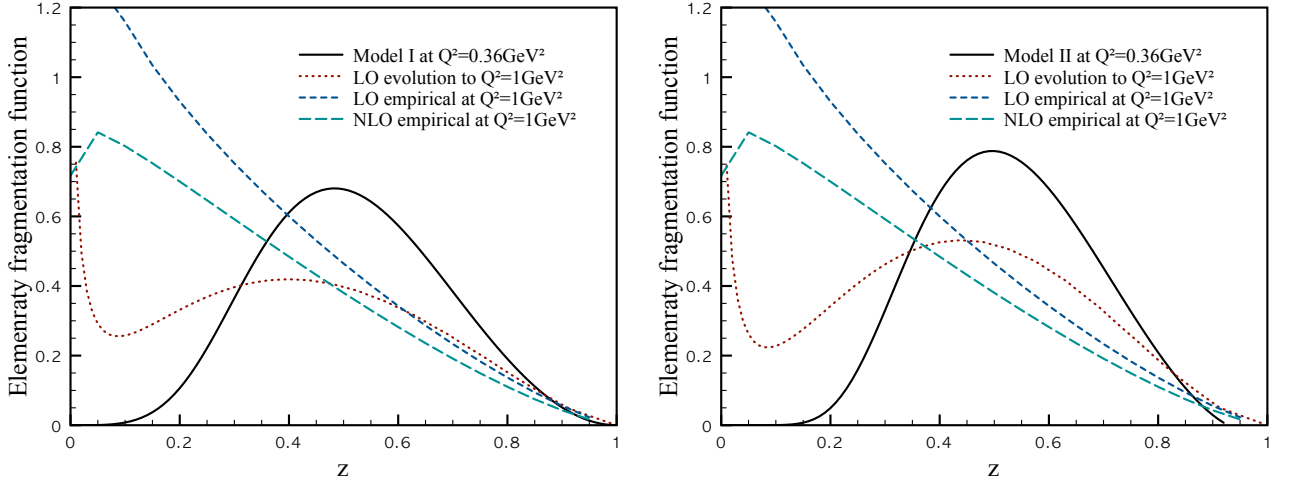


FIG. 4: (Color online) Renormalized elementary fragmentation functions $zD_u^\pi(z)$ at $Q^2 = 0.36 \text{ GeV}^2$ (solid) and they are evolved to $Q^2 = 1 \text{ GeV}^2$ at LO (dotted). The empirical data are taken from Ref. [7] for the LO (dashed) and NLO (long-dashed) analyses at $Q^2 = 1 \text{ GeV}^2$. We present the model I (left) and II (right) results, separately.

parametrized, taking into account that the fragmentation function must be zero at $z = 0$, as follows [7]:

$$D_u^\pi(z) = N_u^\pi z^{\alpha_u^\pi} (1-z)^{\beta_u^\pi}, \quad N_u^\pi = \frac{M_u^\pi}{B(\alpha_u^\pi + 2, \beta_u^\pi + 1)}, \quad (30)$$

where $B(x, y)$ in the denominator stands for the beta function with arguments x and y . The LO and NLO values for α and β , obtained at $Q^2 = 1 \text{ GeV}^2$ are given in Table II following Ref. [7]:

The empirical fragmentation functions at $Q^2 = 1 \text{ GeV}^2$ at LO and NLO are drawn in Figure 4 in the dash and long-dash lines, respectively with the inputs including Eq. (30) and the values listed in Table II. As for Model I (left), the LO and NLO empirical curves are qualitatively matching with the theoretical calculation (dot) for the region $z \gtrsim 0.5$ whereas they deviate considerably in the region $z \lesssim 0.5$. As discussed in Refs. [16, 17], the fragmentation function curves can be enhanced by taking into account the jet contributions in the region $z \lesssim 0.5$. Hence, although we have not considered those contributions here, the discrepancy between the theoretical and empirical curves might be cured by including the jet contributions which are now under progress. [40]. The theoretical curve deviates from the empirical ones even for the region $z \gtrsim 0.5$, if we use Model II as shown in the right panel of Figure 4. From these observations, thus, we can conclude that Model I provides more realistic results than Model II.

We demonstrate our results for the parton distribution functions evolved from $Q^2 = 0.36 \text{ GeV}^2$ (solid) to 4 GeV^2 at LO (dot) and NLO (dash) in Figure 5 for the minus-type (left column) and plus-type (right column). In the upper two panels, we depict the results from Model I, while the results of Model II are represented in the lower two panels. The empirical curves are computed using Eq. (29) and input values in Table III. It is clearly shown that the Model I results are in better agreement with the empirical one for the minus-type distribution, which is nothing but the valance quark distribution function than the Model II ones. We also observe both models underestimates the plus-type distribution functions in the region $x \lesssim 0.2$.

After the evolution, we plot the valance quark distribution function at $Q^2 = 27 \text{ GeV}^2$ in Figure 6 for Model I (solid) and Model II (dot). The data points are taken from Ref. [9]. The Model I result reproduces the data qualitatively excellent as expected from Figure 5, whereas the Model II one deviates from them sizably for whole x region.

	M_u^π (LO)	α_u^π (LO)	β_u^π (LO)	M_u^π (NLO)	α_u^π (NLO)	β_u^π (NLO)
$D_u^\pi(z)$	0.546 ± 0.085	-1.100 ± 0.183	1.282 ± 0.140	0.401 ± 0.052	-0.963 ± 0.177	1.370 ± 0.144

TABLE II: Parameters for the empirical pion fragmentation functions in Eq. (30), evaluated at $Q^2 = 1 \text{ GeV}^2$ for LO and NLO evolutions, in Ref. [7].

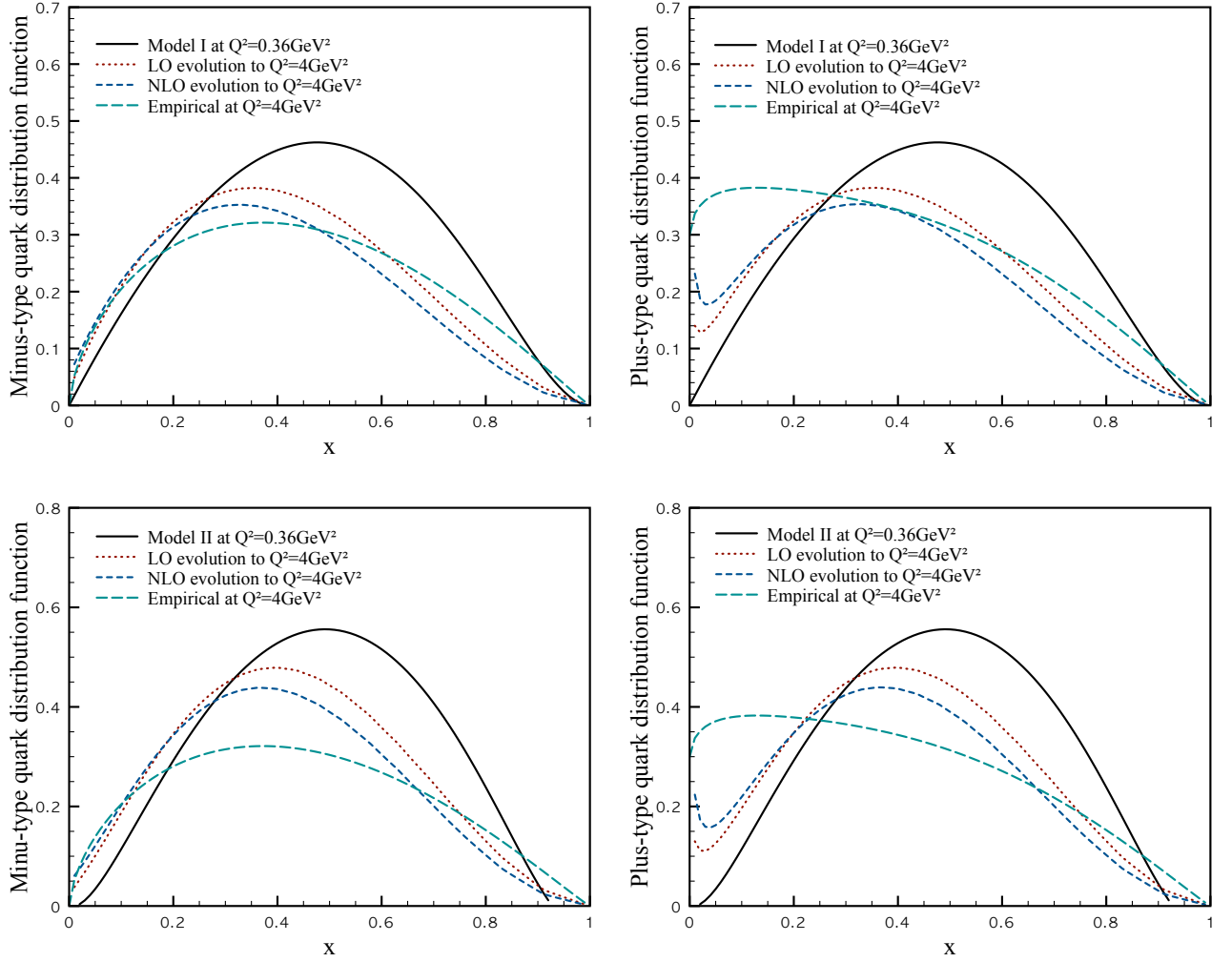


FIG. 5: (Color online) Minus-type $x(f_u^\pi - f_{\bar{u}}^\pi)$ (left column) and plus-type $x(f_u^\pi + f_{\bar{u}}^\pi)$ (right column) quark distribution functions at different Q^2 values, i.e. $Q^2 = (0.36, 4) \text{ GeV}^2$. The Q^2 evolution is performed at LO and NLO. The empirical data are taken from Ref. [10].

IV. SUMMARY AND CONCLUSION

We have studied the fragmentation functions and parton distribution functions for the positively charged pion using NLChQM motivated by the instanton vacuum configuration. We have computed them at the low-renormalization scale $\Lambda^2 \approx Q^2 \approx 0.36 \text{ GeV}^2$, then evolved them up to certain higher Q^2 values by the DGLAP evolution. We performed two separate calculations as Model I and II, depending on the different cutoff schemes for the k_T integration. The numerical results were compared with other models with only local interactions. Below, we list our important observations in this work:

- The fragmentation and parton distribution functions calculated by NLChQM manifest the effects from the nonlocal-interactions between the quarks and the PS mesons. Naturally, if we reduce the nonlocal-interaction into local ones, we can obtain the well-known results such as those from the NJL model. The nonlocal interactions make significant differences in comparison to those from the models with local interactions.

α_ϕ	β_ϕ	A_s^ϕ	η_ϕ
0.64	1.08	0.9	5.0

TABLE III: Input values for the empirical quark distribution function given in Ref. [10].

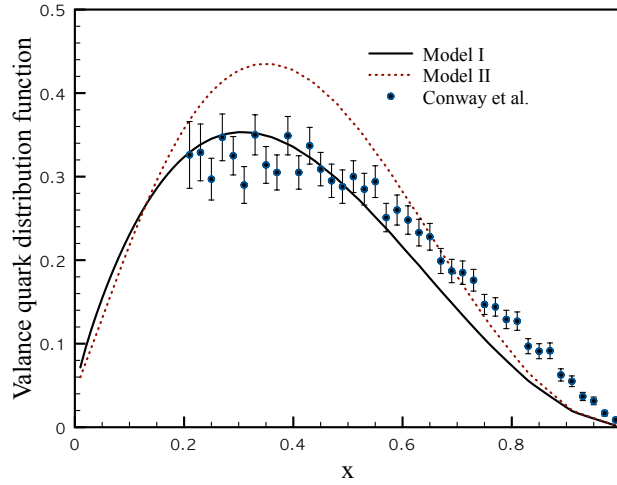


FIG. 6: (Color online) Valence (minus-type) quark distribution function $xf_u^\pi(x)$, computed by model I (solid) and model II (dot) via the DGLAP evolution at LO to $Q^2 = 27 \text{ GeV}^2$. The data are taken from Ref. [9].

- By comparing the renormalization factors $\mathcal{N}_{\pi/u}$ for the renormalized fragmentation functions from all models, the pion-cloud effects turns out to be much more pronounced in NLChQM since the intricate nonlocal quark-PS meson interaction enhances the effects. The NLChQM results behave like a mixture of the PV and PS (NJL) schemes. It can be understood by expanding quark-PS meson coupling term $\sim M_k$ by its momentum k .
- The fragmentation functions from NLChQM are relatively symmetric with respect to z whereas the local interaction models give asymmetric or tilted curves. After high- Q^2 evolution, we find substantial deviations in comparison to the empirical data, in particular, in the small z region. The inclusion of the jet contributions is expected to help to resolve this discrepancy.
- The minus-type (valance) quark distribution function reproduces the empirical data qualitatively well for various Q^2 values, while the plus-type one indicates sizable deviations at small x region. In overall, Model I results are in relatively good agreement with the empirical data. This is rather natural, since Model I is much more consistent theoretical framework than Model II.

As a conclusion, the present nonlocal-interaction model, NLChQM provides very distinctive features, which have not been observed in usual local models, and contains interesting physical implications. We are working with more realistic ingredients, such as the resonance and the hadron-jet contributions, and appear elsewhere. The extension of the present theoretical framework to the flavor SU(3) octet mesons for the kaons is also under progress.

Acknowledgments

We are grateful to J. W. Chen and H. Kohyama for fruitful discussions. We also thank A. Metz for his very helpful communications. S.i.N. is very grateful to the hospitality during his staying at National Taiwan University (NTU) with the financial support from NCTS (North) in Taiwan, where the present work was initiated. The work of C.W.K. was supported by the grant NSC 99-2112-M-033-004-MY3 from National Science Council (NSC) of Taiwan. He has also acknowledged the support of NCTS (North) in Taiwan.

-
- [1] J. C. Collins, Nucl. Phys. **B396**, 161-182 (1993).
 - [2] P. J. Mulders, R. D. Tangerman, Nucl. Phys. **B461**, 197-237 (1996).
 - [3] D. Boer, P. J. Mulders, Phys. Rev. **D57**, 5780-5786 (1998).
 - [4] M. Anselmino, M. Boglione, F. Murgia, Phys. Lett. **B362**, 164-172 (1995).
 - [5] S. D. Drell, D. J. Levy, T. -M. Yan, Phys. Rev. **187**, 2159-2171 (1969).
 - [6] S. Kretzer, Phys. Rev. **D62**, 054001 (2000). [hep-ph/0003177].

- [7] M. Hirai, S. Kumano, T. H. Nagai and K. Sudoh, Phys. Rev. D **75**, 094009 (2007).
- [8] B. A. Kniehl, G. Kramer, B. Potter, Nucl. Phys. **B582**, 514-536 (2000).
- [9] J. S. Conway et al., Phys. Rev. **D39**, 92-122 (1989).
- [10] P. J. Sutton, A. D. Martin, R. G. Roberts, W. J. Stirling, Phys. Rev. **D45**, 2349-2359 (1992).
- [11] X.D. Ji and Z. K. Zhu, hep-ph/9402303v2.
- [12] A. Bacchetta, R. Kundu, A. Metz and P. J. Mulders, Phys. Rev. D **65**, 094021 (2002).
- [13] D. Amrath, A. Bacchetta and A. Metz, Phys. Rev. D **71**, 114018 (2005).
- [14] S. Meissner, A. Metz and D. Pitonyak, Phys. Lett. B **690**, 296 (2010).
- [15] W. Bentz, T. Hama, T. Matsuki, K. Yazaki, Nucl. Phys. **A651**, 143-173 (1999).
- [16] T. Ito, W. Bentz, I. -Ch. Cloet, A. W. Thomas and K. Yazaki, Phys. Rev. D **80**, 074008 (2009).
- [17] H. H. Matevosyan, A. W. Thomas and W. Bentz, Phys. Rev. D **83**, 114010 (2011).
- [18] T. Nguyen, A. Bashir, C. D. Roberts, P. C. Tandy, Phys. Rev. **C83**, 062201 (2011).
- [19] R. Aloisio, V. Berezinsky, M. Kachelriess, Phys. Rev. **D69**, 094023 (2004).
- [20] A. E. Dorokhov, Nuovo Cim. A **109**, 391 (1996).
- [21] M. Praszalowicz and A. Rostworowski, Phys. Rev. D **66**, 054002 (2002).
- [22] S. i. Nam and H. -Ch. Kim, Phys. Rev. D **74**, 076005 (2006).
- [23] S. i. Nam, H. -Ch. Kim, A. Hosaka and M. M. Musakhanov, Phys. Rev. D **74**, 014019 (2006).
- [24] E. V. Shuryak, Nucl. Phys. B **203**, 93 (1982).
- [25] D. Diakonov and V. Y. Petrov, Nucl. Phys. B **272**, 457 (1986).
- [26] D. Diakonov and V. Y. Petrov, Nucl. Phys. B **245**, 259 (1984).
- [27] T. Schäfer and E. V. Shuryak, Rev. Mod. Phys. **70**, 323 (1998).
- [28] D. Diakonov, Prog. Part. Nucl. Phys. **51**, 173 (2003).
- [29] M. Musakhanov, Eur. Phys. J. **C9**, 235 (1999).
- [30] M. Musakhanov, Nucl. Phys. A **699**, 340 (2002).
- [31] S. i. Nam and H. -Ch. Kim, Phys. Rev. D **77**, 094014 (2008).
- [32] S. i. Nam and H. -Ch. Kim, Phys. Lett. B **700**, 305 (2011).
- [33] A. E. Dorokhov, L. Tomio, Phys. Rev. **D62**, 014016 (2000).
- [34] A. E. Dorokhov, JETP Lett. **77**, 63-67 (2003). [hep-ph/0212156].
- [35] J. W. Negele, Nucl. Phys. Proc. Suppl. **73**, 92 (1999).
- [36] P. O. Bowman, U. M. Heller, D. B. Leinweber, A. G. Williams, Nucl. Phys. Proc. Suppl. **119**, 323-325 (2003).
- [37] M. Botje, Comput. Phys. Commun. **182**, 490 (2011).
- [38] The QCD-evolution fortran program QCDNUM17, written by M. Botje, at <http://www.nikhef.nl/user/h24/qcdnum>.
- [39] G. P. Lepage and S. J. Brodsky, Phys. Rev. D **22**, 2157 (1980).
- [40] S. i. Nam and C. W. Kao, in preparation.